Estimation of small failure probabilities by partially Bayesian active learning line sampling: Theory and algorithm

Chao Dang[a,*], Marcos A. Valdebenito[b], Jingwen Song[c], Pengfei Wei[d], Michael Beer[a,e,f]

[a] *Institute for Risk and Reliability, Leibniz University Hannover, Callinstr. 34, Hannover 30167, Germany*
[b] *Chair for Reliability Engineering, TU Dortmund University, Leonhard-Euler-Str. 5, Dortmund 44227, Germany*
[c] *School of Mechanical Engineering, Northwestern Polytechnical University, Xi'an 710072, PR China*
[d] *School of Power and Energy, Northwestern Polytechnical University, Xi'an 710072, PR China*
[e] *Institute for Risk and Uncertainty, University of Liverpool, Liverpool L69 7ZF, United Kingdom*
[f] *International Joint Research Center for Resilient Infrastructure & International Joint Research Center for Engineering Reliability and Stochastic Mechanics, Tongji University, Shanghai 200092, PR China*

Abstract

Line sampling (LS) has proved to be a highly promising advanced simulation technique for assessing small failure probabilities. Despite the great interest in practical engineering applications, many efforts from the research community have been devoted to improving the standard LS. This paper aims at offering some new insights into the LS method, leading to an innovative method, termed 'partially Bayesian active learning line sampling' (PBAL-LS). The problem of evaluating the failure probability integral in the LS method is treated as a Bayesian, rather than frequentist, inference problem, which allows to incorporate our prior knowledge and model the discretization error. The Gaussian process model is used as a prior distribution, and the posterior mean, and an upper bound of the posterior variance of the failure probability are derived. Based on the posterior statistics of the failure probability, we also put forward a learning function and a stopping criterion, which enable us to use active learning. Besides, an efficient algorithm is also designed to implement the PBAL-LS method, with the ability to automatically adjust the important direction and efficiently process the lines. Five numerical examples are studied to demonstrate the performance of the proposed PBAL-LS method against several existing methods.

Keywords:

Line sampling; Failure probability; Bayesian inference; Active Learning; Gaussian process

*Corresponding author
Email address: chao.dang@irz.uni-hannover.de (Chao Dang)

1. Introduction

Structural reliability analysis has been recognized as a central task for the design and analysis of safety-critical engineering systems in the presence of uncertainties, since the pioneering work of Freudenthal [1] in 1956. For more than half a century, great efforts have been devoted to developing suitable methods to assess the so-called failure probability. Since most engineering systems are expected to be highly reliable, failure should be a rare event, and therefore the probability of failure should be sufficiently small. Besides, very often the failure probability analysis involves evaluating a computationally intensive model multiple times. Among various numerical methods proposed in literature to address the computational challenges, stochastic simulation techniques hold a prominent position. Examples of such techniques include the direct Monte Carlo simulation (MCS) method [2], Importance Sampling [3, 4], Directional Sampling [5], Subset Simulation (SubSim) [6, 7], Line Sampling (LS) [8, 9], etc. However, it is usually computationally expensive to directly apply these stochastic simulation methods. This promotes the development of surrogate-assisted stochastic simulation, e.g., efficient global reliability analysis [10] and AK-MCS (active learning Kriging-MCS) [11]. In this study, we will restrict ourselves to the LS method and its variants.

As a stand-alone simulation technique, the preliminary idea of LS appeared in a talk [12], and then evolved into an expanded version that is normally known to us in [8]. Note that a similar but not quite the same method, known as axis orthogonal sampling, was introduced earlier in [13]. The underlying idea behind LS is to employ lines, instead of random points, to probe the failure domain. At implementation level, a so-called 'important direction' that points towards the failure domain is first required to be identified, and then one has to solve a number of one-dimensional reliability problems conditional on the random line samples parallel to the important direction. The failure probability is finally obtained as an average of the failure probabilities along all the lines. The LS method has proved to be a highly promising approach to evaluating small failure probabilities of weakly or moderately nonlinear problems, which can be found in a number of practical cases. It has been successfully applied to various areas of engineering, such as aerospace [14, 15], automotive [16], nuclear [17, 18] and civil engineering [19, 20], etc. Besides, the standard LS method is also available in a general-purpose software suite for uncertainty quantification and risk management, called

COSSAN [21].

In recent years, increasing attention from the research community has been devoted to expanding the application scope of the original LS method and further improving its performance. As far as the first aspect is concerned, the standard LS method with possible modifications has been used for non-original purposes, such as sensitivity analysis [22, 23, 24, 25], estimation of failure probability function or its bounds in the context of reliability-based design optimization [26] and polymorphic uncertainty propagation [27, 28, 29, 30]. The second aspect consists of, e.g., adapting the important direction [27, 31], reformulating the LS estimator [31, 32], processing the lines sequentially [27] and introducing multiple important directions [33]. To reduce the computational burden for expensive reliability analysis, surrogate models, such as artificial neural network [18] and Gaussian process (also known as Kriging) [34, 35, 36], have also been combined with LS. As a representative, the adaptive Gaussian process regression - line sampling (APGR-LS) method [36] has shown to be capable of assessing very small failure probabilities with a reduced number of performance function evaluations. However, the practical performance of APGR-LS is dependent on a good important direction that is determined by the first-order reliability method, which may suffer from non-convergence and unnecessary computational demands. Besides, it also has a hard-to-tune parameter that is closely related to the learning function and stopping criterion. One can refer to [37] for the recent advancements of the LS method.

The objective of this work is to provide some new insights into the LS method mainly from the perspective of Bayesian active learning, at least partially. More specifically, we develop an innovative LS method, called 'partially Bayesian active learning line sampling' (PBAL-LS). The main contributions of the present work can be summarized as follows. First, the problem of evaluating the failure probability integral in the LS method is reinterpreted by a Bayesian, rather than frequentist, inference problem for the first time. This will enable to incorporate our prior knowledge about the function we wish to learn, which is not allowed for frequentist inference. Second, we present a principled Bayesian approach that is able to reflect our epistemic uncertainty about the failure probability stemming from the discretization error. In this context, the Gaussian process is used as a prior distribution. The induced posterior statistics of the failure probability is derived. Third,

the Bayesian approach is further cast in an active learning setting. Two essential components, namely learning function and stopping criterion, are proposed based on the uncertainty representation of the failure probability. Fourth, we also offer a tailored algorithm for implementing the PBAL-LS in a strategic manner. Two novel features of the algorithm are the adaption of important direction and efficient line processing.

The rest of the paper is structured as follows. Section 2 briefly reviews the standard LS method, followed by a discussion on its limitations. Theoretical aspects of the proposed PBAL-LS method are given in Section 3. In Section 4, we present the proposed PBAL-LS algorithm in a step-by-step manner. Five benchmark examples are investigated in Section 5 to demonstrate the developed method. The paper ends with some concluding remarks in Section 6.

2. Brief review of the standard line sampling

In this section, we revisit the standard LS method after introducing the failure probability definition in the standard normal space. Besides, the key factors affecting the practical performance of the standard LS method are also identified and discussed, as they motivate us to offer a partially Bayesian active learning counterpart in Section 3 and its algorithm in Section 4.

2.1. Failure probability definition in standard normal space

Let $\boldsymbol{X} = X_1, X_2, \cdots, X_d] \in \mathcal{X} \subseteq \mathbb{R}^d$ denote a vector of d physical random variables, which are used to model the uncertain inputs of a performance function $g : \mathcal{X} \to \mathcal{Y}$ associated with the behavior of a system. It is assumed that these physical random variables have a known jointed probability density function (PDF), which is denoted as $f_{\boldsymbol{X}}(\boldsymbol{x})$. In addition, a failure event occurs whenever the performance function takes a value smaller than zero, i.e., $y = g(\boldsymbol{x}) < 0$. It is important to note that for most cases of practical interest the performance function is an expensive-to-evaluate black box, and non-Gaussian inputs might be encountered. Due to the latter, without loss of generality we further assume that $\boldsymbol{X}$ is a vector containing d non-Gaussian random variables. As the LS method typically operates in the standard normal space, it is of necessity to transform the vector $\boldsymbol{X}$ into a standard normal one $\boldsymbol{U} = [U_1, U_2, \cdots, U_d] \in \mathcal{U} \subseteq \mathbb{R}^d$ using an appropriate method (e.g., iso-probabilistic transformation, Nataf transformation and Rosenblatt transformation, etc.).

Such transformation is denoted by $\boldsymbol{U} = T(\boldsymbol{X}) : \mathcal{X} \to \mathcal{U}$, and hence the transformed performance function with respect to $\boldsymbol{U}$ is given by $Z = \mathcal{G}(\boldsymbol{U}) : \mathcal{U} \to \mathcal{Z}$ such that $\mathcal{G} = g \circ T^{-1}$, where $T^{-1} : \mathcal{U} \to \mathcal{X}$ represents the inverse transformation. Under these settings, the failure probability P_F can be defined as:

$$P_F = \int_{\mathbb{R}^d} I_{\mathcal{G}}(\boldsymbol{u}) \phi_{\boldsymbol{U}}(\boldsymbol{u}) \mathrm{d}\boldsymbol{u}, \tag{1}$$

where $I_{\mathcal{G}}(\boldsymbol{u})$ is the failure indicator function corresponding to $\mathcal{G}$: $I_{\mathcal{G}}(\boldsymbol{u}) = 1$ if $\mathcal{G}(\boldsymbol{u}) < 0$ and $I_{\mathcal{G}}(\boldsymbol{u}) = 0$ otherwise; $\phi_{\boldsymbol{U}}(\boldsymbol{u})$ is the joint PDF of $\boldsymbol{U}$, i.e., $\phi_{\boldsymbol{U}}(\boldsymbol{u}) = \prod_{i=1}^{d} \phi_{U_i}(u_i) = \frac{1}{(2\pi)^{d/2}} \exp\left(-\frac{\boldsymbol{u}\boldsymbol{u}^{\mathrm{T}}}{2}\right)$, where $(\cdot)^{\mathrm{T}}$ denotes transpose.

2.2. Failure probability estimation by line sampling

The basic idea of LS is to reformulate the d-dimensional failure probability integral defined in Eq. (1) into a nested integral, with the inner being a one-dimensional integral along an important direction $\boldsymbol{\alpha}$, and the outer being a $(d-1)$-dimensional integral over a hyperplane orthogonal to $\boldsymbol{\alpha}$ [12, 8]. The so-called important direction $\boldsymbol{\alpha}$ is a unit vector that points towards the failure domain $F = \{\boldsymbol{u} \in \mathcal{U} : \mathcal{G}(\boldsymbol{u}) < 0\}$. In practical implementation, several strategies have been suggested to choose an important direction, e.g., the normalized gradient vector of the $\mathcal{G}$-function at a certain point [14] and the unit vector pointing towards the design point [38]. Once $\boldsymbol{\alpha}$ is given, the original standard normal vector $\boldsymbol{U}$ can be expressed in a new orthogonal coordinate system such that:

$$\boldsymbol{U} = U^{\parallel}\boldsymbol{\alpha} + \boldsymbol{U}^{\perp}\boldsymbol{r}, \tag{2}$$

where $\boldsymbol{r}$ is a $(d-1) \times d$ matrix consisting of $d-1$ orthogonal basis vectors of the hyperplane perpendicular to $\boldsymbol{\alpha}$; $U^{\parallel}$ is a standard normal variable and $\boldsymbol{U}^{\perp}$ is a $(d-1)$-dimensional standard normal vector because of the rotational invariance of the standard normal vector. In the new orthogonal coordinate system, the failure probability defined in Eq. (1) can be rewritten as:

$$\begin{aligned} P_F &= \int_{\mathbb{R}^{d-1}} \int_{\mathbb{R}} I_{\mathcal{G}}(u^{\parallel}\boldsymbol{\alpha} + \boldsymbol{u}^{\perp}\boldsymbol{r}) \phi_{U^{\parallel}}(u^{\parallel}) \phi_{\boldsymbol{U}^{\perp}}(\boldsymbol{u}^{\perp}) \mathrm{d}u^{\parallel} \mathrm{d}\boldsymbol{u}^{\perp} \\ &= \int_{\mathbb{R}^{d-1}} \left(\int_{\mathbb{R}} I_{\mathcal{G}}(u^{\parallel}\boldsymbol{\alpha} + \boldsymbol{u}^{\perp}\boldsymbol{r}) \phi_{U^{\parallel}}(u^{\parallel}) \mathrm{d}u^{\parallel} \right) \phi_{\boldsymbol{U}^{\perp}}(\boldsymbol{u}^{\perp}) \mathrm{d}\boldsymbol{u}^{\perp}, \end{aligned} \tag{3}$$

where $\phi_{U^{\parallel}}(u^{\parallel})$ and $\phi_{\boldsymbol{U}^{\perp}}(\boldsymbol{u}^{\perp})$ are the (joint) PDF of $U^{\parallel}$ and $\boldsymbol{U}^{\perp}$, respectively. Under the assumption that the failure domain is simply a half-open region (see Fig. 1), the inner integral in Eq. (3) is equal to $\Phi(-\beta(\boldsymbol{u}^{\perp}))$, where $\beta(\boldsymbol{u}^{\perp})$ denotes the Euclidean distance between the limit state surface $\mathcal{G}=0$ and a point $\boldsymbol{u}^{\perp}$ on the orthogonal hyperplane along the direction $\boldsymbol{\alpha}$. In this case, Eq. (3) can be further simplified as:

$$P_F = \int_{\mathbb{R}^{d-1}} \Phi(-\beta(\boldsymbol{u}^{\perp}))\phi_{\boldsymbol{U}^{\perp}}(\boldsymbol{u}^{\perp})\mathrm{d}\boldsymbol{u}^{\perp}. \tag{4}$$

Note that in Eq. (4) P_F is actually defined as an expectation of $\Phi(-\beta(\boldsymbol{U}^{\perp}))$ with respect to the standard normal vector $\boldsymbol{U}^{\perp}$. In addition, since the previous presumption is often the case for most component reliability problems with linear, weakly nonlinear or moderately nonlinear performance functions, Eq. (4) rather than Eq. (3) is commonly used in literature. Thereafter, we also refer to Eq. (4) when mentioning LS, unless otherwise specified.

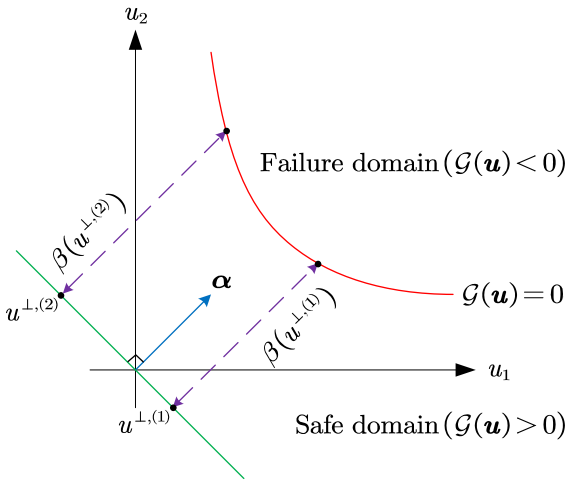

Figure 1: Schematic illustration of the standard LS in two dimensions.

In the standard LS method, the failure probability integral defined in Eq. (4) is solved by mainly using a purely frequentist procedure – MCS method. The MCS estimator of P_F is given by:

$$\hat{P}_F = \frac{1}{N}\sum_{i=1}^{N} \Phi(-\beta(\boldsymbol{u}^{\perp,(i)})), \tag{5}$$

where $\left\{\boldsymbol{u}^{\perp,(i)}\right\}_{i=1}^{N}$ is a set of N random samples drawn from $\phi_{\boldsymbol{U}^{\perp}}(\boldsymbol{u}^{\perp})$; $\beta(\boldsymbol{u}^{\perp,(i)})$ is the distance between $\boldsymbol{u}^{\perp,(i)}$ and the limit state surface $\mathcal{G}=0$ along the important direction $\boldsymbol{\alpha}$, as illustrated in Fig. 1. To

avoid the specification of $\boldsymbol{r}$, a convenient way is to directly obtain $\boldsymbol{u}^{\perp,(i)}\boldsymbol{r}$ rather than $\boldsymbol{u}^{\perp,(i)}$ by $\boldsymbol{u}^{\perp,(i)}\boldsymbol{r} = \boldsymbol{u}^{(i)} - (\boldsymbol{\alpha}\cdot\boldsymbol{u}^{(i)})\boldsymbol{\alpha}$, where $\boldsymbol{u}^{(i)}$ is a random sample generated according to $\phi_{\boldsymbol{U}}(\boldsymbol{u})$. The term $\beta(\boldsymbol{u}^{\perp,(i)})$ can be solved by means of any appropriate root-finding algorithms, such as polynomial interpolation [14] and Newton's method [27]. Note that for each $\boldsymbol{u}^{\perp,(i)}$ finding the value $\beta(\boldsymbol{u}^{\perp,(i)})$ usually requires a handful of $\mathcal{G}$-function evaluations. The variance associated with the MCS estimator is:

$$\sigma^2_{\hat{P}_F} = \frac{1}{N(N-1)}\sum_{i=1}^{n}\left(\Phi(-\beta(\boldsymbol{u}^{\perp,(i)})) - \hat{P}_F\right)^2. \tag{6}$$

In general, the practical performance of the standard LS method is affected by three main aspects. The first aspect consists in the choice of the important direction $\boldsymbol{\alpha}$. A good choice will lead to a fast convergence rate of the subsequent MCS procedure, and hence reduces the sample size N. However, this in turn requires a good knowledge of the limit state surface, which is usually at the expense of many additional $\mathcal{G}$-function evaluations. Another aspect is associated with the MCS method used to solve Eq. (4). In case that a poor important direction is chosen and/or the variance of $\Phi(-\beta(\boldsymbol{U}^{\perp}))$ is significant, a large size N is required for the MCS method to achieve a desirable level of accuracy. What is more, the MCS method as a typical frequentist approach suffers from several major limitations, e.g., brute force feature and inability to incorporate prior knowledge, though it has many undeniable advantages. As for the last aspect, the accuracy and efficiency related to searching each $\beta(\boldsymbol{u}^{\perp,(i)})$ may also influence the overall performance of the standard LS method.

3. Partially Bayesian active learning line sampling: Theory

In view of the limitations of the standard LS method, especially when examined from frequentist interpretation, we offer a Bayesian active learning treatment in this section, at least partially. The resulting methodology is termed 'partially Bayesian active learning line sampling' (PBAL-LS). Our objective here is to approximate the intractable integral in Eq. (4) from a Bayesian active learning perspective, under the premise that a suitable important direction has been determined. However, the premise is only for convenience and not necessary in practice, as shown in Section 4. The key to achieving the objective relies on

approaching the problem of evaluating the integral in Eq. (4) using Bayesian inference, as opposed to frequentist inference. By doing so, it is possible to incorporate our prior knowledge and model the discretization error. Such a Bayesian idea is actually consistent with the spirit of a class of Bayesian probabilistic numerical methods, i.e., Bayesian probabilistic numerical integration [39, 40]. Further, the Bayesian treatment makes it possible to address the underlying problem in an active learning manner.

3.1. Prior distribution

Recall that the class of reliability problems we are interested in the present study involves only weakly to mildly nonlinear behavior. In other words, the limit state surface $\mathcal{G}(\boldsymbol{u}) = 0$ is not expected to be extremely rough, and hence the distance function $\beta(\boldsymbol{u}^{\perp})$ exhibits a smooth behavior. Our prior beliefs about $\beta(\boldsymbol{u}^{\perp})$ can thus be reflected by defining a proper prior distribution over it. A popular choice for a prior distribution over functions is a Gaussian process (GP) due to its conjugate properties and modelling power. In this study, we also assume a GP prior for $\beta(\boldsymbol{u}^{\perp})$, which is expressed as:

$$\hat{\beta}_0(\boldsymbol{u}^{\perp}) \sim \mathcal{GP}(m_{\hat{\beta}_0}(\boldsymbol{u}^{\perp}), k_{\hat{\beta}_0}(\boldsymbol{u}^{\perp}, \boldsymbol{u}^{\perp\prime})), \tag{7}$$

where $\hat{\beta}_0$ denotes the prior distribution of β; $m_{\hat{\beta}_0}(\boldsymbol{u}^{\perp})$ and $k_{\hat{\beta}_0}(\boldsymbol{u}^{\perp}, \boldsymbol{u}^{\perp\prime})$ denote respectively the prior mean and covariance functions, by which the GP model is completely specified. The prior mean function reflects our expected value of $\beta(\boldsymbol{u}^{\perp})$, while the prior covariance function encodes our key assumptions about $\beta(\boldsymbol{u}^{\perp})$, such as smoothness or periodicity. For convenience and without loss of generality, in this study the prior mean function is chosen as a constant denoted as b and the prior covariance function is assumed to be the squared exponential kernel:

$$m_{\hat{\beta}_0}(\boldsymbol{u}^{\perp}) = b, \tag{8}$$

$$k_{\hat{\beta}_0}(\boldsymbol{u}^{\perp}, \boldsymbol{u}^{\perp\prime}) = \sigma_f^2 \exp\left(-\frac{1}{2}(\boldsymbol{u}^{\perp} - \boldsymbol{u}^{\perp\prime})\boldsymbol{\Sigma}^{-1}(\boldsymbol{u}^{\perp} - \boldsymbol{u}^{\perp\prime})^{\mathrm{T}}\right), \tag{9}$$

where $\sigma_f > 0$ is the process standard deviation; $\boldsymbol{\Sigma} = \mathrm{diag}\{l_1, l_2, \cdots, l_d\}$ with $l_i > 0$ being the characteristic length scale in i-th dimension; $\mathrm{diag}\{\cdot\}$ means to form a square diagonal matrix with its arguments on the main diagonal. All these parameters $\{b, \sigma_f, l_1, l_2, \cdots, l_d\}$ are collectively referred to as hyperparameters.

3.2. Hyperparameters tuning and posterior statistics

Given a observation dataset $\boldsymbol{\mathcal{D}} = \left\{\boldsymbol{\mathcal{U}}^{\perp}, \boldsymbol{\mathcal{H}}\right\}$, where $\boldsymbol{\mathcal{U}}^{\perp} = \left\{\boldsymbol{u}^{\perp,(i)}\right\}_{i=1}^{n}$ is an n-by-$(d-1)$ matrix with $\boldsymbol{u}^{\perp,(i)}$ being the i-th observing location and $\boldsymbol{\mathcal{H}} = \left[h^{(1)}, h^{(2)}, \cdots, h^{(n)}\right]^{\mathrm{T}}$ is an n-by-1 vector with i-th element being $h^{(i)} = \beta(\boldsymbol{u}^{\perp,(i)})$. The hyper-parameters can be learned from the observed data $\boldsymbol{\mathcal{D}}$ by some suitable methods, e.g., maximum likelihood estimation [41].

The posterior distribution of β conditioning the GP prior in Eq. (7) on $\boldsymbol{\mathcal{D}}$ is again a GP:

$$\hat{\beta}_n(\boldsymbol{u}^{\perp}) \sim \mathcal{GP}(m_{\hat{\beta}_n}(\boldsymbol{u}^{\perp}), k_{\hat{\beta}_n}(\boldsymbol{u}^{\perp}, \boldsymbol{u}^{\perp\prime})), \tag{10}$$

where $\hat{\beta}_n$ denotes the posterior distribution of β conditioned on $\boldsymbol{\mathcal{D}}$; $m_{\hat{\beta}_n}(\boldsymbol{u}^{\perp})$ and $k_{\hat{\beta}_n}(\boldsymbol{u}^{\perp}, \boldsymbol{u}^{\perp\prime})$ are the posterior mean and covariance functions of β, which can be given by:

$$m_{\hat{\beta}_n}(\boldsymbol{u}^{\perp}) = m_{\hat{\beta}_0}(\boldsymbol{u}^{\perp}) + \boldsymbol{k}_{\beta_0}(\boldsymbol{u}^{\perp}, \boldsymbol{\mathcal{U}}^{\perp})^{\mathrm{T}} \boldsymbol{K}_{\beta_0}(\boldsymbol{\mathcal{U}}^{\perp}, \boldsymbol{\mathcal{U}}^{\perp})^{-1} (\boldsymbol{\mathcal{H}} - \boldsymbol{m}_{\hat{\beta}_0}(\boldsymbol{\mathcal{U}}^{\perp})), \tag{11}$$

$$k_{\hat{\beta}_n}(\boldsymbol{u}^{\perp}, \boldsymbol{u}^{\perp\prime}) = k_{\hat{\beta}_0}(\boldsymbol{u}^{\perp}, \boldsymbol{u}^{\perp\prime}) - \boldsymbol{k}_{\beta_0}(\boldsymbol{u}^{\perp}, \boldsymbol{\mathcal{U}}^{\perp})^{\mathrm{T}} \boldsymbol{K}_{\beta_0}(\boldsymbol{\mathcal{U}}^{\perp}, \boldsymbol{\mathcal{U}}^{\perp})^{-1} \boldsymbol{k}_{\beta_0}(\boldsymbol{\mathcal{U}}^{\perp}, \boldsymbol{u}^{\perp\prime}), \tag{12}$$

where $\boldsymbol{m}_{\hat{\beta}_0}(\boldsymbol{\mathcal{U}}^{\perp})$ is an n-by-1 mean vector with i-th element being $m_{\hat{\beta}_0}(\boldsymbol{u}^{\perp,(i)})$; $\boldsymbol{k}_{\beta_0}(\boldsymbol{u}^{\perp}, \boldsymbol{\mathcal{U}}^{\perp})$ is an n-by-1 covariance vector with i-th element being $k_{\hat{\beta}_0}(\boldsymbol{u}^{\perp}, \boldsymbol{u}^{\perp,(i)})$; $\boldsymbol{k}_{\beta_0}(\boldsymbol{\mathcal{U}}^{\perp}, \boldsymbol{u}^{\perp\prime})$ is an n-by-1 covariance vector with i-th element being $\boldsymbol{k}_{\beta_0}(\boldsymbol{u}^{\perp,(i)}, \boldsymbol{u}^{\perp\prime})$; $\boldsymbol{K}_{\beta_0}(\boldsymbol{\mathcal{U}}^{\perp}, \boldsymbol{\mathcal{U}}^{\perp})$ is an n-by-n covariance matrix with (i,j)-th entry being $k_{\beta_0}(\boldsymbol{u}^{\perp,(i)}, \boldsymbol{u}^{\perp,(j)})$.

The GP posterior of β as shown in Eq. (10) can be employed together with the normal cumulative distribution function to produce a posterior on $\Phi(-\beta)$. However, the induced posterior distribution $\hat{\Phi}_n(-\hat{\beta})$ of $\Phi(-\beta)$ is not exactly known in closed form. Fortunately, the posterior mean and variance functions that are needed in the present work can be derived as follows:

$$\begin{aligned} m_{\hat{\Phi}_n(-\hat{\beta})}\left(\boldsymbol{u}^{\perp}\right) =& \mathbb{E}_{\hat{\beta}_n}\left[\hat{\Phi}\left(-\hat{\beta}_n\left(\boldsymbol{u}^{\perp}\right)\right)\right] \\ =& \mathbb{E}_U\left[\hat{\Phi}\left(-\left(m_{\hat{\beta}_n}\left(\boldsymbol{u}^{\perp}\right) + \sigma_{\hat{\beta}_n}\left(\boldsymbol{u}^{\perp}\right) U\right)\right)\right] \\ =& \Phi\left(\frac{-m_{\hat{\beta}_n}\left(\boldsymbol{u}^{\perp}\right)}{\sqrt{1+\sigma^2_{\hat{\beta}_n}\left(\boldsymbol{u}^{\perp}\right)}}\right), \end{aligned} \tag{13}$$

$$
\begin{aligned}
\sigma^2_{\hat{\Phi}_n(-\hat{\beta})}\left(\boldsymbol{u}^{\perp}\right) =& \mathbb{V}_{\hat{\beta}_n}\left[\hat{\Phi}\left(-\hat{\beta}_n\left(\boldsymbol{u}^{\perp}\right)\right)\right] \\
=& \mathbb{E}_{\hat{\beta}_n}\left[\hat{\Phi}^2\left(-\hat{\beta}_n\left(\boldsymbol{u}^{\perp}\right)\right)\right] - \mathbb{E}_{\hat{\beta}_n}\left[\hat{\Phi}\left(-\hat{\beta}_n\left(\boldsymbol{u}^{\perp}\right)\right)\right]^2 \\
=& \mathbb{E}_U\left[\hat{\Phi}^2\left(-\left(m_{\hat{\beta}_n}\left(\boldsymbol{u}^{\perp}\right) + \sigma_{\hat{\beta}_n}\left(\boldsymbol{u}^{\perp}\right)U\right)\right)\right] - \Phi^2\left(\frac{-m_{\hat{\beta}_n}\left(\boldsymbol{u}^{\perp}\right)}{\sqrt{1+\sigma^2_{\hat{\beta}_n}\left(\boldsymbol{u}^{\perp}\right)}}\right) \\
=& \Phi\left(\frac{-m_{\hat{\beta}_n}\left(\boldsymbol{u}^{\perp}\right)}{\sqrt{1+\sigma^2_{\hat{\beta}_n}\left(\boldsymbol{u}^{\perp}\right)}}\right) - 2\mathcal{T}\left(\frac{-m_{\hat{\beta}_n}\left(\boldsymbol{u}^{\perp}\right)}{\sqrt{1+\sigma^2_{\hat{\beta}_n}\left(\boldsymbol{u}^{\perp}\right)}}, \frac{1}{\sqrt{1+2\sigma^2_{\hat{\beta}_n}\left(\boldsymbol{u}^{\perp}\right)}}\right) - \Phi^2\left(\frac{-m_{\hat{\beta}_n}\left(\boldsymbol{u}^{\perp}\right)}{\sqrt{1+\sigma^2_{\hat{\beta}_n}\left(\boldsymbol{u}^{\perp}\right)}}\right) \\
=& \Phi\left(\frac{-m_{\hat{\beta}_n}\left(\boldsymbol{u}^{\perp}\right)}{\sqrt{1+\sigma^2_{\hat{\beta}_n}\left(\boldsymbol{u}^{\perp}\right)}}\right)\Phi\left(\frac{m_{\hat{\beta}_n}\left(\boldsymbol{u}^{\perp}\right)}{\sqrt{1+\sigma^2_{\hat{\beta}_n}\left(\boldsymbol{u}^{\perp}\right)}}\right) - 2\mathcal{T}\left(\frac{-m_{\hat{\beta}_n}\left(\boldsymbol{u}^{\perp}\right)}{\sqrt{1+\sigma^2_{\hat{\beta}_n}\left(\boldsymbol{u}^{\perp}\right)}}, \frac{1}{\sqrt{1+2\sigma^2_{\hat{\beta}_n}\left(\boldsymbol{u}^{\perp}\right)}}\right),
\end{aligned}
\tag{14}
$$

where $\mathbb{E}_{\hat{\beta}_n}[\cdot]$ and $\mathbb{V}_{\hat{\beta}_n}[\cdot]$ denote the expectation and variance operators taken with respect to $\hat{\beta}_n$; $\mathbb{E}_U[\cdot]$ denotes the expectation operator taken with respect to the standard normal variable U; $\sigma_{\hat{\beta}_n}\left(\boldsymbol{u}^{\perp}\right)$ is the posterior standard function of β, i.e., $\sigma_{\hat{\beta}_n}\left(\boldsymbol{u}^{\perp}\right) = \sqrt{k_{\hat{\beta}_n}(\boldsymbol{u}^{\perp}, \boldsymbol{u}^{\perp})}$; $\mathcal{T}(\cdot,\cdot)$ is the Owen's T function, which is defined by an analytically intractable integral. Note that the above derivation makes partial use of the results in [42].

The posterior distribution of $\Phi(-\beta)$ will give arise to a posterior distribution of P_F via the integral operator. Since $\hat{\Phi}_n(-\hat{\beta})$ is not known in closed form, we cannot arrive at the exact posterior distribution $\hat{P}_{F,n}$. This, however, does not impose significant restrictions on the proposed method because the low-order moments other than the exact distribution could be more useful. Analogous to the results of previous studies (e.g., [43]), the posterior mean and variance of P_F turn out to be:

$$
\begin{aligned}
m_{\hat{P}_{F,n}} =& \mathbb{E}_{\boldsymbol{U}^{\perp}}\left[m_{\hat{\Phi}_n(-\hat{\beta})}\left(\boldsymbol{U}^{\perp}\right)\right] \\
=& \int_{\mathbb{R}^{d-1}} \Phi\left(\frac{-m_{\hat{\beta}_n}\left(\boldsymbol{u}^{\perp}\right)}{\sqrt{1+\sigma^2_{\hat{\beta}_n}\left(\boldsymbol{u}^{\perp}\right)}}\right)\phi_{\boldsymbol{U}^{\perp}}(\boldsymbol{u}^{\perp})\mathrm{d}\boldsymbol{u}^{\perp},
\end{aligned}
\tag{15}
$$

$$
\begin{aligned}
\sigma^2_{\hat{P}_{F,n}} =& \mathbb{E}_{\boldsymbol{U}^{\perp},\boldsymbol{U}^{\perp\prime}}\left[k_{\hat{\Phi}_n(-\hat{\beta})}(\boldsymbol{U}^{\perp}, \boldsymbol{U}^{\perp\prime})\right] \\
=& \int_{\mathbb{R}^{d-1}}\int_{\mathbb{R}^{d-1}} k_{\hat{\Phi}_n(-\hat{\beta})}(\boldsymbol{u}^{\perp}, \boldsymbol{u}^{\perp\prime})\phi_{\boldsymbol{U}^{\perp}}(\boldsymbol{u}^{\perp})\phi_{\boldsymbol{U}^{\perp\prime}}(\boldsymbol{u}^{\perp\prime})\mathrm{d}\boldsymbol{u}^{\perp}\mathrm{d}\boldsymbol{u}^{\perp\prime},
\end{aligned}
\tag{16}
$$

where $\mathbb{E}_{\boldsymbol{U}^{\perp}}[\cdot]$ means to take expectation of its argument with respect to $\boldsymbol{U}^{\perp}$; $\mathbb{E}_{\boldsymbol{U}^{\perp},\boldsymbol{U}^{\perp\prime}}[\cdot]$ denotes the expectation taken with respect to $\boldsymbol{U}^{\perp}$ and $\boldsymbol{U}^{\perp\prime}$ ($\boldsymbol{U}^{\perp}$ and $\boldsymbol{U}^{\perp\prime}$ are independent and identically distributed);

$k_{\hat{\Phi}_n(-\hat{\beta})}(\boldsymbol{u}^{\perp}, \boldsymbol{u}^{\perp\prime})$ is the posterior covariance function of $\Phi(-\beta)$. Eq. (15) implies that the posterior mean of P_F is the expectation of the posterior mean function of $\Phi(-\beta)$ taken with respect to $\boldsymbol{U}^{\perp}$, while Eq. (16) suggests that the posterior variance of P_F is the expectation of the posterior covariance function of $\Phi(-\beta)$ taken with respect to $\boldsymbol{U}^{\perp}$ and $\boldsymbol{U}^{\perp\prime}$. However, as the posterior covariance function of $\Phi(-\beta)$ is unknown, we cannot arrive at the solution to the posterior variance of P_F. To circumvent this issue, our proposal is to consider an upper-bound of $\sigma^2_{\hat{P}_{F,n}}$. Using the Cauchy–Schwarz inequality (i.e., $k_{\hat{\Phi}_n(-\hat{\beta})}(\boldsymbol{u}^{\perp}, \boldsymbol{u}^{\perp\prime}) \leq \sigma_{\hat{\Phi}_n(-\hat{\beta})}\left(\boldsymbol{u}^{\perp}\right) \sigma_{\hat{\Phi}_n(-\hat{\beta})}\left(\boldsymbol{u}^{\perp\prime}\right)$), we have

$$\begin{aligned}\sigma^2_{\hat{P}_{F,n}} \leq \overline{\sigma}^2_{\hat{P}_{F,n}} &= \int_{\mathbb{R}^{d-1}} \int_{\mathbb{R}^{d-1}} \sigma_{\hat{\Phi}_n(-\hat{\beta})}\left(\boldsymbol{u}^{\perp}\right) \sigma_{\hat{\Phi}_n(-\hat{\beta})}\left(\boldsymbol{u}^{\perp\prime}\right) \phi_{\boldsymbol{U}^{\perp}}(\boldsymbol{u}^{\perp}) \phi_{\boldsymbol{U}^{\perp\prime}}(\boldsymbol{u}^{\perp\prime}) \mathrm{d}\boldsymbol{u}^{\perp} \mathrm{d}\boldsymbol{u}^{\perp\prime} \\ &= \left(\int_{\mathbb{R}^{d-1}} \sqrt{ \Phi\left(\frac{-m_{\hat{\beta}_n}(\boldsymbol{u}^{\perp})}{\sqrt{1+\sigma^2_{\hat{\beta}_n}(\boldsymbol{u}^{\perp})}} \right) \Phi\left(\frac{m_{\hat{\beta}_n}(\boldsymbol{u}^{\perp})}{\sqrt{1+\sigma^2_{\hat{\beta}_n}(\boldsymbol{u}^{\perp})}} \right) - 2\mathcal{T}\left(\frac{-m_{\hat{\beta}_n}(\boldsymbol{u}^{\perp})}{\sqrt{1+\sigma^2_{\hat{\beta}_n}(\boldsymbol{u}^{\perp})}}, \frac{1}{\sqrt{1+2\sigma^2_{\hat{\beta}_n}(\boldsymbol{u}^{\perp})}} \right) } \right. \\ &\quad \left. \times \phi_{\boldsymbol{U}^{\perp}}(\boldsymbol{u}^{\perp}) \mathrm{d}\boldsymbol{u}^{\perp} \right)^2, \end{aligned} \tag{17}$$

where $\overline{\sigma}^2_{\hat{P}_{F,n}}$ denotes the resulting upper bound of $\sigma^2_{\hat{P}_{F,n}}$ and the equality holds if and only if $\hat{\Phi}_n(-\hat{\beta})$ between any two locations is linearly dependent. The posterior mean $m_{\hat{P}_{F,n}}$ in Eq. (15) can be used as a natural estimate for P_F, whereas $\overline{\sigma}^2_{\hat{P}_{F,n}}$ in Eq. (17) can measure our maximum possible epistemic uncertainty about the estimate. The epistemic uncertainty is related to the numerical uncertainty arising from the fact that the β-function is only observed at a number of discrete points. As we only offer an upper bound for quantifying the numerical uncertainty (as revealed by Eq. (17)), the proposed approach is termed as *partially* Bayesian.

3.3. Learning function and stopping criterion

Our general goal with the PBAL-LS method is to produce a failure probability estimate with a desired degree of accuracy using as few β-function evaluations as possible. To achieve such goal, one potential strategy is to implement the Bayesian approach sequentially. Specifically, an active learning procedure can be readily used in conjunction with the Bayesian framework. An essential ingredient for an active learning procedure is a so-called learning (acquisition) function that can suggest the best next observation point based on our prior knowledge. In this work, a new learning function that is extracted from $\overline{\sigma}_{\hat{P}_{F,n}}$, called

upper-bound posterior standard deviation contribution (UPSDC), is proposed as follows:

$$\mathrm{UPSDC}\left(\boldsymbol{u}^{\perp}\right)=\sqrt{\Phi\left(\frac{-m_{\hat{\beta}_n}\left(\boldsymbol{u}^{\perp}\right)}{\sqrt{1+\sigma^2_{\hat{\beta}_n}\left(\boldsymbol{u}^{\perp}\right)}}\right)\Phi\left(\frac{m_{\hat{\beta}_n}\left(\boldsymbol{u}^{\perp}\right)}{\sqrt{1+\sigma^2_{\hat{\beta}_n}\left(\boldsymbol{u}^{\perp}\right)}}\right)-2\mathcal{T}\left(\frac{-m_{\hat{\beta}_n}\left(\boldsymbol{u}^{\perp}\right)}{\sqrt{1+\sigma^2_{\hat{\beta}_n}\left(\boldsymbol{u}^{\perp}\right)}},\frac{1}{\sqrt{1+2\sigma^2_{\hat{\beta}_n}\left(\boldsymbol{u}^{\perp}\right)}}\right)}\times\phi_{\boldsymbol{U}^{\perp}}(\boldsymbol{u}^{\perp}). \tag{18}$$

It is easy to check that $\overline{\sigma}_{\hat{P}_{F,n}}=\int_{\mathbb{R}^{d-1}}\mathrm{UPSDC}\left(\boldsymbol{u}^{\perp}\right)\mathrm{d}\boldsymbol{u}^{\perp}$ holds. Therefore, the UPSDC function can be seen as a measure of the contribution of epistemic uncertainty at the site $\boldsymbol{u}^{\perp}$ to the upper bound of the posterior standard deviation of P_F. The best next point $\boldsymbol{u}^{\perp,(n+1)}$ where to query the β-function can be selected as the point maximizing the UPSDC function (i.e., $\boldsymbol{u}^{\perp,(n+1)}=\arg\max_{\boldsymbol{u}^{\perp}\in\mathcal{U}^{\perp}}\mathrm{UPSDC}\left(\boldsymbol{u}^{\perp}\right)$), which is expected to reduce $\overline{\sigma}_{\hat{P}_{F,n+1}}$ the most. Another key ingredient for an active learning procedure is associated with a stopping criterion that can determine when to stop the iteration. In this study, the stopping criterion is defined as whether the upper-bound of the posterior COV of the failure probability $\overline{\mathrm{COV}}_{\hat{P}_{F,n}}$ is less than a tolerance ϵ:

$$\overline{\mathrm{COV}}_{\hat{P}_{F,n}}=\frac{\overline{\sigma}_{\hat{P}_{F,n}}}{m_{\hat{P}_{F,n}}}<\epsilon, \tag{19}$$

where ϵ is user-specified. A smaller ϵ typically implies a higher accuracy of $m_{\hat{P}_{F,n}}$, but with increased computational cost, and vice versa.

4. Partially Bayesian active learning line sampling: Algorithm

In this section, we present an efficient algorithm for applying the proposed PBAL-LS method to practical reliability analysis problems, where several important implementation issues are addressed. The first issue is related to the choice of the important direction $\boldsymbol{\alpha}$ that is assumed to be already known before the Bayesian treatment in the preceding section, which, however, should be appropriately specified in practice. Instead of a fixed and initially determined one, an adaptive strategy is proposed to adjust the important direction on the fly throughout the simulation. As for the second issue, searching for the distance between a given sample $\boldsymbol{u}^{\perp}$ and the limit state surface $\mathcal{G}=0$ along the important direction, is tackled in a strategic manner. The third issue arising from coping with $m_{\hat{P}_{F,n}}$, $\overline{\sigma}^2_{\hat{P}_{F,n}}$ and $\mathrm{UPSDC}\left(\boldsymbol{u}^{\perp}\right)$ is also properly processed from a numerical point of view.

The proposed algorithm for the PBAL-LS method is illustrated with the flowchart in Fig. 3, and it consists of six main steps described as below. Note that for clarity the core tasks of each step are listed in the blue box, followed by detailed descriptions when necessary.

Step 1: Selection of an initial important direction

An initial important direction $\boldsymbol{\alpha}^{(0)}$ must be chosen in this step, and then one has to specify the corresponding matrix $\boldsymbol{r}^{(0)}$ for the hyperplane orthogonal to $\boldsymbol{\alpha}^{(0)}$.

The important direction will be designed to be updated automatically as soon as a more probable one is found, and hence the proposed algorithm does not need to start with an optimal important direction. As a rough guess, the initial important direction can be selected as the negative normalized gradient of the $\mathcal{G}$-function at the origin:

$$\boldsymbol{\alpha}^{(0)} = -\frac{\nabla_{\boldsymbol{u}}\mathcal{G}(\mathbf{0})}{||\nabla_{\boldsymbol{u}}\mathcal{G}(\mathbf{0})||}, \tag{20}$$

where $\nabla_{\boldsymbol{u}}\mathcal{G}(\mathbf{0}) = \left[\frac{\partial\mathcal{G}(\mathbf{0})}{\partial u_1}, \frac{\partial\mathcal{G}(\mathbf{0})}{\partial u_2}, \cdots, \frac{\partial\mathcal{G}(\mathbf{0})}{\partial u_d}\right]$; $||\cdot||$ denotes the Euclidean norm. Note that $\boldsymbol{\alpha}^{(0)}$ corresponds to the direction of steepest descent of the $\mathcal{G}$-function at the origin, and is expected to point towards the failure domain for those cases we are interested in. As the $\mathcal{G}$-function is assumed to be known only implicitly with respect to $\boldsymbol{u}$, forward difference is used to estimate $\nabla_{\boldsymbol{u}}\mathcal{G}(\mathbf{0})$ at the expense of $(d+1)$ $\mathcal{G}$-function evaluations.

The matrix $\boldsymbol{r}^{(0)}$ is theoretically not unique given $\boldsymbol{\alpha}^{(0)}$. In practice, however, it needs to be specified from numerical point of view. To do so, one can resort to, e.g., the Gram–Schmidt process, which is also used in the following steps whenever needed.

Step 2: Generation of an initial observation dataset

This step involves generating a small initial observation dataset $\boldsymbol{\mathcal{D}} = \left\{\boldsymbol{\mathcal{U}}^{\perp}, \boldsymbol{\mathcal{H}}\right\}$ and updating the important direction if possible at the same time.

First, an auxiliary line is deployed from the origin along the direction $\boldsymbol{\alpha}^{(0)}$ (denoted as $u^{\parallel}\boldsymbol{\alpha}^{(0)}$), and

we have to find the solution to the equation $\mathcal{G}(u^{\parallel}\boldsymbol{\alpha}^{(0)}) = 0$. Note that since this line is only designed for providing a rough reference for the following procedure, an accurate solution to $\mathcal{G}(u^{\parallel}\boldsymbol{\alpha}^{(0)}) = 0$ is not necessary. To this end, it is suggested to use a simple interpolation method, e.g., piecewise cubic Hermite interpolating polynomial (PCHIP). The PCHIP method requires evaluating the $\mathcal{G}$-function at three discrete points of $u^{\parallel}$. In this study, the three points are specified as $c_1 = 3$, $c_2 = 6$ and $c_3 = 8$. The interpolated value of $u^{\parallel}$ is denoted as $\beta^{(0)}$. The interpolation procedure is illustrated in Fig. 2(a).

Second, the β-function should be observed at several locations so as to form an initial observation dataset and update the important direction if possible. A small number, n_0, of samples $\left\{\boldsymbol{u}^{\perp,(j)}\right\}_{j=1}^{n_0}$ are generated from $\phi_{\boldsymbol{U}^{\perp}}(\boldsymbol{u}^{\perp})$ by using, e.g., Sobol sequence. In this study, n_0 is set to be 5. Here, the Newton's method is used to identify the root of $\mathcal{G}(u^{\parallel,(j)}\boldsymbol{\alpha}^{(l)} + \boldsymbol{u}^{\perp,(j)}\boldsymbol{r}^{(l)}) = 0$. Instead of processing $\left\{\boldsymbol{u}^{\perp,(j)}\right\}_{j=1}^{n_0}$ in the order as they are generated, we rearrange them according to the distance from the origin in ascending order, denoted as $\left\{\tilde{\boldsymbol{u}}^{\perp,(j)}\right\}_{j=1}^{n_0}$. By doing so, one can make use of $\beta^{(0)}$ as the starting point when searching $\tilde{h}^{(1)}$, and $\tilde{h}^{(j)}$ for $\tilde{h}^{(j+1)}$ $(j = 1, 2, \cdots, n_0)$. The intersection point for the line $\tilde{u}^{\parallel,(j)}\boldsymbol{\alpha}^{(l)} + \tilde{\boldsymbol{u}}^{\perp,(j)}\boldsymbol{r}^{(l)}$ with the limit state surface $\mathcal{G}(\boldsymbol{u}) = 0$ is recorded as $\tilde{\boldsymbol{u}}^{(j)} = \tilde{h}^{(j)}\boldsymbol{\alpha}^{(l)} + \tilde{\boldsymbol{u}}^{\perp,(j)}\boldsymbol{r}^{(l)}$. Whenever a nearest intersection point from the origin is found, e.g., $||\tilde{\boldsymbol{u}}^{(j)}|| = \min_{j=1}^{j} ||\tilde{\boldsymbol{u}}^{(j)}||$ $(j \geq 2)$, the important direction should be immediately updated as $\boldsymbol{\alpha}^{(l+1)} = \frac{\tilde{\boldsymbol{u}}^{(j)}}{||\tilde{\boldsymbol{u}}^{(j)}||}$, together with $\boldsymbol{r}^{(l+1)}$. One can refer to Figs. 2(b) and 2(c) for a schematic illustration. Once all the lines have been processed, $\boldsymbol{\mathcal{U}}^{\perp}$ can be obtained by projecting the intersection points $\left\{\tilde{\boldsymbol{u}}^{(j)}\right\}_{j=1}^{n_0}$ onto the last orthogonal hyperplane, and $\boldsymbol{\mathcal{H}}$ contains the corresponding distances between $\left\{\tilde{\boldsymbol{u}}^{(j)}\right\}_{j=1}^{n_0}$ and the last orthogonal hyperplane along the last importance direction.

Step 3: Computation of posterior statistics of the failure probability

> Conditional on the observation dataset $\boldsymbol{\mathcal{D}}$, the posterior mean and upper bound on the posterior standard deviation of the failure probability are evaluated.

The GP posterior of β conditional on $\boldsymbol{\mathcal{D}}$ can be obtained analytically as defined in Eq. (10). This process can be done with the help of existing software packages, e.g., *fitrgp* function in Statistics and Machine Learning Toolbox of Matlab.

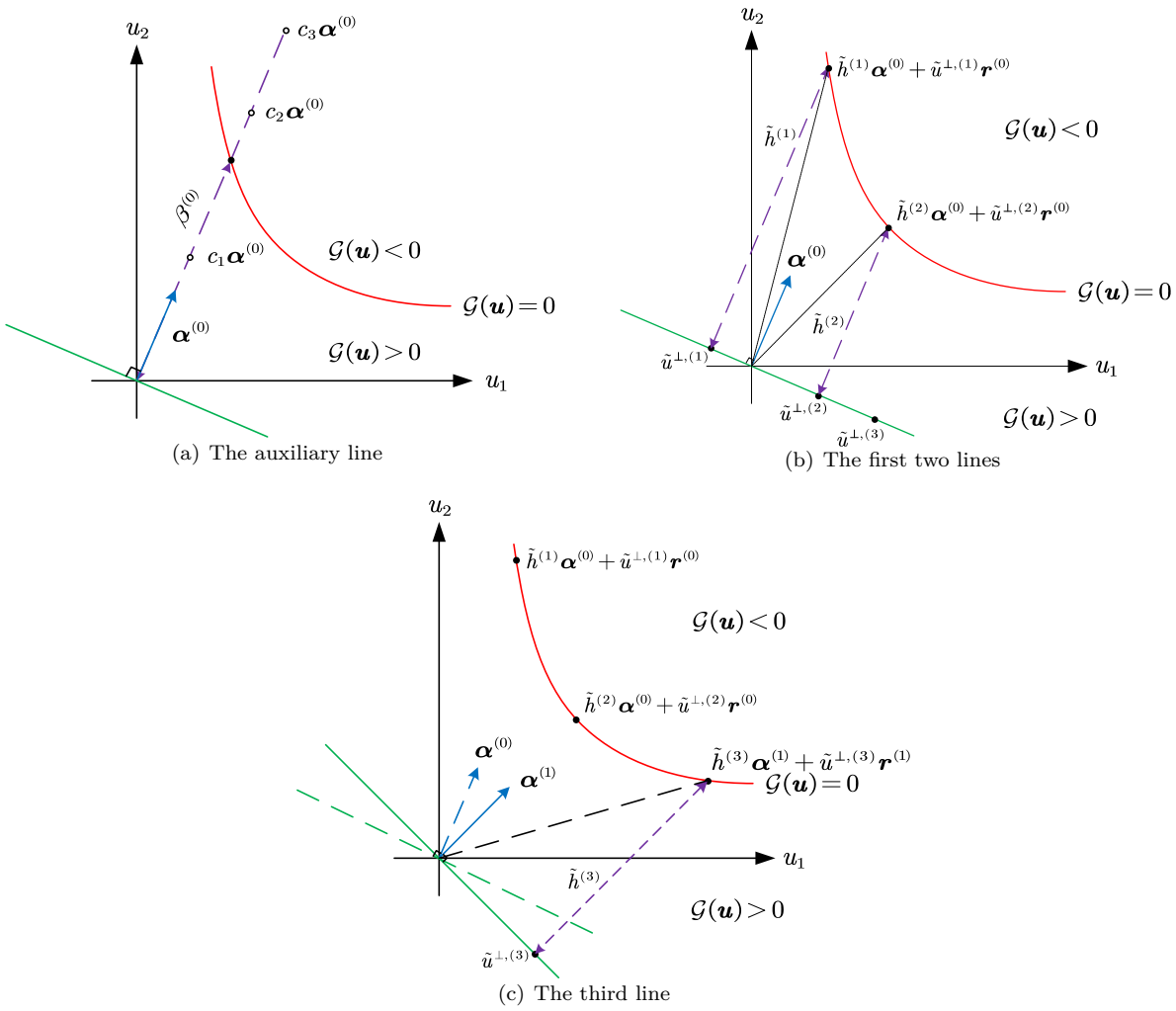

Figure 2: Illustration of Step 2 of the proposed PBAL-LS algorithm in two dimensions ($n_0 = 3$).

As can be seen in Eqs. (15) and (17), the posterior mean and upper bound of the posterior standard deviation of the failure probability are not analytically tractable. In view of that, the MCS method is used here. According to Eq. (15), an unbiased estimator for the posterior mean of the failure probability is given by:

$$\hat{m}_{\hat{P}_{F,n}} = \frac{1}{N}\sum_{i=1}^{N} \Phi\left(\frac{-m_{\hat{\beta}_n}\left(\boldsymbol{u}^{\perp,(i)}\right)}{\sqrt{1+\sigma^2_{\hat{\beta}_n}\left(\boldsymbol{u}^{\perp,(i)}\right)}}\right), \tag{21}$$

where $\left\{\boldsymbol{u}^{\perp,(i)}\right\}_{i=1}^{N}$ is a set of N random samples generated from $\phi_{\boldsymbol{U}^{\perp}}(\boldsymbol{u}^{\perp})$. The variance of the estimator

can be expressed as:

$$\mathbb{V}\left[\hat{m}_{\hat{P}_{F,n}}\right] = \frac{1}{N(N-1)} \sum_{i=1}^{N} \left[\Phi\left(\frac{-m_{\hat{\beta}_n}\left(\boldsymbol{u}^{\perp,(i)}\right)}{\sqrt{1+\sigma^2_{\hat{\beta}_n}\left(\boldsymbol{u}^{\perp,(i)}\right)}} \right) - \hat{m}_{\hat{P}_{F,n}} \right]^2. \tag{22}$$

The estimator for the upper bound on the posterior standard deviation of the failure probability is formulated as:

$$\hat{\bar{\sigma}}_{\hat{P}_{F,n}} = \frac{1}{N} \sum_{i=1}^{N} \sqrt{ \mathbb{E}_U\left[\hat{\Phi}^2\left(-\left(m_{\hat{\beta}_n}\left(\boldsymbol{u}^{\perp,(i)}\right) + \sigma_{\hat{\beta}_n}\left(\boldsymbol{u}^{\perp,(i)}\right) U \right) \right) \right] - \Phi^2\left(\frac{-m_{\hat{\beta}_n}\left(\boldsymbol{u}^{\perp,(i)}\right)}{\sqrt{1+\sigma^2_{\hat{\beta}_n}\left(\boldsymbol{u}^{\perp,(i)}\right)}} \right)}. \tag{23}$$

It should be pointed out that we do not make use of the final result of $\sigma^2_{\hat{\Phi}_n(-\hat{\beta})}\left(\boldsymbol{u}^{\perp}\right)$ (but the intermediate result) to formulate $\hat{\bar{\sigma}}_{\hat{P}_{F,n}}$ because the involved Owen's T function is not easy to handle numerically. Instead, the expectation term in Eq. (23) can be readily approximated by some well-known quadrature rules available in a number of software packages, e.g., the *integral* function in Matlab. The variance of the estimator in Eq. (23) is written as:

$$\mathbb{V}\left[\hat{\bar{\sigma}}_{\hat{P}_{F,n}}\right] = \frac{1}{N(N-1)} \sum_{i=1}^{N} \left[\sqrt{ \mathbb{E}_U\left[\hat{\Phi}^2\left(-\left(m_{\hat{\beta}_n}\left(\boldsymbol{u}^{\perp,(i)}\right) + \sigma_{\hat{\beta}_n}\left(\boldsymbol{u}^{\perp,(i)}\right) U \right) \right) \right] - \Phi^2\left(\frac{-m_{\hat{\beta}_n}\left(\boldsymbol{u}^{\perp,(i)}\right)}{\sqrt{1+\sigma^2_{\hat{\beta}_n}\left(\boldsymbol{u}^{\perp,(i)}\right)}} \right)} - \hat{\bar{\sigma}}_{\hat{P}_{F,n}} \right]^2. \tag{24}$$

To ensure the accuracy of $\hat{m}_{\hat{P}_{F,n}}$ and $\hat{\bar{\sigma}}_{\hat{P}_{F,n}}$, the sample size N should be large enough. However, a too large sample size may lead to low efficiency and even memory loss when evaluating $\hat{m}_{\hat{P}_{F,n}}$ and $\hat{\bar{\sigma}}_{\hat{P}_{F,n}}$. For this reason, it is suggested to increase the sample size progressively until a stopping criterion is satisfied. A convenient stopping criterion is defined as the maximum value of two COVs ($\sqrt{\mathbb{V}\left[\hat{m}_{\hat{P}_{F,n}}\right]}\Big/\hat{m}_{\hat{P}_{F,n}}$ and $\sqrt{\mathbb{V}\left[\hat{\bar{\sigma}}_{\hat{P}_{F,n}}\right]}\Big/\hat{\bar{\sigma}}_{\hat{P}_{F,n}}$), i.e., $\max\left(\sqrt{\mathbb{V}\left[\hat{m}_{\hat{P}_{F,n}}\right]}\Big/\hat{m}_{\hat{P}_{F,n}}, \sqrt{\mathbb{V}\left[\hat{\bar{\sigma}}_{\hat{P}_{F,n}}\right]}\Big/\hat{\bar{\sigma}}_{\hat{P}_{F,n}} \right) < \delta$, where δ is the tolerance. In this study, δ is set to be 2%.

Step 4: Judgment of the stopping condition on learning

The stopping criterion for active learning should be examined and then decide whether to continue or stop the algorithm.

If $\hat{\overline{\mathrm{COV}}}_{\hat{P}_{F,n}} = \hat{\bar{\sigma}}_{\hat{P}_{F,n}}/\hat{m}_{\hat{P}_{F,n}} < \epsilon$ is satisfied twice in a row, go to **Step 6**; otherwise, go to **Step 5**. The tolerance ϵ can take a value between $5\% - 10\%$.

Step 5: Active updating of the observation dataset

The β-function is observed at a new point identified by our learning function. Then, the important direction can be modified if possible and the previous observation dataset can be updated.

The next best point to query the β-function is identified by maximizing the proposed UPSDC function such that:

$$\boldsymbol{u}^{\perp,(n+1)} = \underset{\boldsymbol{u}^{\perp}\in\mathcal{U}^{\perp}}{\arg\max} \sqrt{\mathbb{E}_U\left[\hat{\Phi}^2\left(-\left(m_{\hat{\beta}_n}\left(\boldsymbol{u}^{\perp}\right)+\sigma_{\hat{\beta}_n}\left(\boldsymbol{u}^{\perp}\right)U\right)\right)\right]-\Phi^2\left(\frac{-m_{\hat{\beta}_n}\left(\boldsymbol{u}^{\perp}\right)}{\sqrt{1+\sigma^2_{\hat{\beta}_n}\left(\boldsymbol{u}^{\perp}\right)}}\right)} \times \phi_{\boldsymbol{U}^{\perp}}(\boldsymbol{u}^{\perp}). \quad (25)$$

It is worth mentioning that the UPSDC function is used in the form given by Eq. (25) rather than Eq. (18) in order to avoid directly dealing with the Owen's T function. The expectation term on the right-hand side of Eq. (25) can be approximated by a suitable quadrature rule, while Eq. (25) can be solved by some nature-inspired optimization algorithms.

The distance $\tilde{h}^{(n+1)}$ between $\boldsymbol{u}^{\perp,(n+1)}$ and the limit state surface $\mathcal{G}=0$ along the latest important direction is searched by the Newton's method. To accelerate the search process, $m_{\hat{\beta}_n}(\boldsymbol{u}^{\perp,(n+1)})$ can be taken as a good starting point. Once $\tilde{h}^{(n+1)}$ is available, it is trivial to obtain the corresponding intersection point $\tilde{\boldsymbol{u}}^{(n+1)}$. If $||\tilde{\boldsymbol{u}}^{(n+1)}|| \neq \min_{j=1}^{n+1}||\tilde{\boldsymbol{u}}^{(j)}||$, the previous training dataset is enriched with $\left\{\boldsymbol{u}^{\perp,(n+1)}, \tilde{h}^{(n+1)}\right\}$; otherwise, the important direction is updated as the normalized $\frac{\tilde{\boldsymbol{u}}^{(n+1)}}{||\tilde{\boldsymbol{u}}^{(n+1)}||}$ (as well as the matrix $\boldsymbol{r}$), and the observation dataset should be renewed by projecting these $n+1$ intersection points onto the latest orthogonal hyperplane. Go to **Step 3**.

Step 6: End of the proposed PBAL-LS algorithm

Return the last estimate of the posterior mean of the failure probability and end the proposed PBAL-LS algorithm.

Note that the important direction might be adapted in both **Step 2** and **Step 5**, which do not require any additional evaluations of the $\mathcal{G}$-function. Similar ideas can be found in several improved LS methods

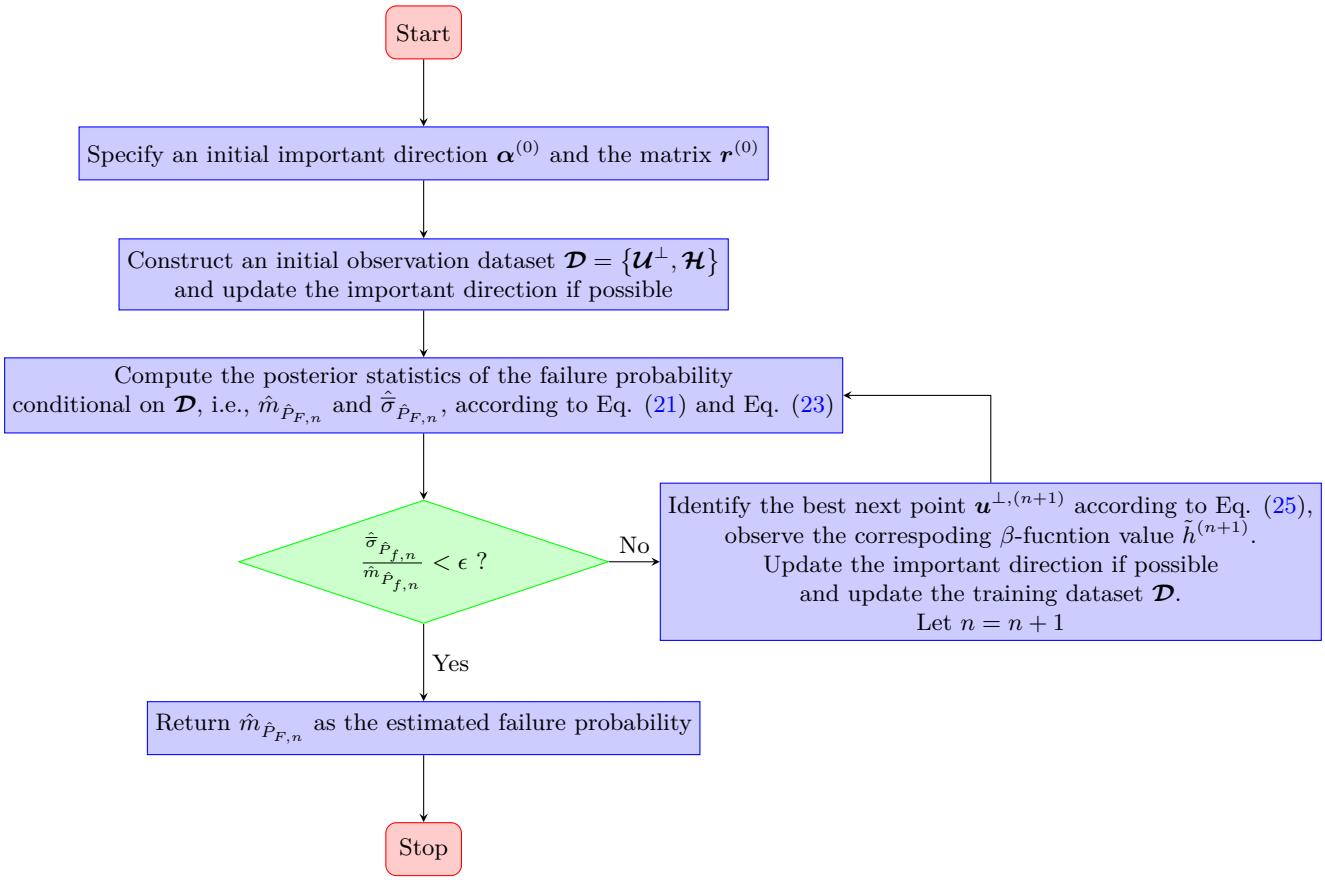

Figure 3: Flowchart of the proposed PBAL-LS algorithm.

[27, 31, 32]. This feature proves to be useful as one does not need to waste extra effort on specifying an optimal important direction. In the active learning process the next location to observe the β-function is chosen in terms of the learning function rather than randomly, which makes the fullest possible use of our prior knowledge about the β-function, and hence can reduce the number of lines required. In addition, the root-finding procedure in **Step 2** is also tailored as information can be reused to accelerate convergence and reduce the number of $\mathcal{G}$-function calls. The authors of [27] adopted a similar but slightly different strategy. In **Step 5**, the starting point of the root-finding algorithm is provided by the GP prediction, and hence incorporating our prior knowledge. It is also worth mentioning that the final result of Eq. (14) and Eq. (18) can be directly used in the PBAL-LS algorithm once an appropriate quadrature rule is available to deal with the Owen's T function.

5. Numerical examples

In this section, the performance of the proposed PBAL-LS method for assessing small failure probabilities is demonstrated against several existing methods by means of five numerical examples. These selected methods include the standard LS [8], combination line sampling (CLS) [32], active learning Kriging - importance sampling (AK-IS) [44] and AGPR-LS [36]. The (initial) important direction is specified by the negative normalized gradient of the g-function at the origin for LS and CLS, while by first-order reliability method using Hasofer-Lind-Rackwitz-Fiessler [45] for and AK-IS and AGPR-LS. The studied numerical examples represent a class of moderately nonlinear problems with varying complexity where those LS methods are expected to be applicable.The common feature of these examples is that they are designed to have very small failure probabilities. In all numerical examples, the MCS method with a sufficiently large sample size is employed to provide the reference failure probability if applicable.

5.1. Example 1: An illustrative problem

The first example involves an illustrative problem with the performance function:

$$Y = g(\boldsymbol{X}) = a - X_2 + bX_1^3 + c\sin\left(dX_1\right), \tag{26}$$

where X_1 and X_2 are two independent standard normal variables; a, b, c and d are four constant parameters, which are specified as: $a = 5.0$, $b = 0.01$, $c = 1.0$ and $d = 1.0$.

The proposed PBAL-LS method is compared in Table 1 with several other methods, including MCS, standard LS, CLS, AK-IS and AGPR-LS. The reference value of the failure probability is obtained as 5.87×10^{-6} (with a COV being 0.41%), provided by the MCS method with 10^{10} samples. It is clear that the LS methods without using the GP model (i.e., standard LS and CLS) require a large number of lines and performance function evaluations in order to produce failure probability estimates with small COVs. AK-IS and AGPR-LS can significantly reduce the number of calls to the performance function, while yielding acceptable failure probability estimates. The performance of the AGPR-LS method, however, is highly dependent upon the parameter ϵ, which is not easy to tune. The proposed method gives the same failure

probability as the AGPR-LS method. However, it requires fewer performance function evaluations than the AGPR-LS method.

For the sake of illustration, Fig. 4 depicts the initial and final important directions, and the intersection points identified by the proposed PBAL-LS method ($\epsilon = 10\%$), along with the true limit state curve. It is shown that the initial important direction chosen by Eq. (20) is far from optimal, but the final one is nearly optimal. Besides, the approximate intersection points are located on the true limit state curve, indicating the accuracy of the root-finding algorithm.

Table 1: Reliability results for Example 1 obtained from several methods.

Method	$\hat{P}_f$	COV$[\hat{P}_f]$ or $\overline{\text{COV}}[\hat{P}_f]$	N_{line}	N_{total}
MCS	5.87×10^{-6}	0.41%	-	10^{10}
Standard LS	6.68×10^{-6}	47.72%	100	721
	6.00×10^{-6}	13.46%	1000	7079
CLS	6.18×10^{-6}	7.68%	100	524
	5.92×10^{-6}	2.36%	1000	5103
AK-IS	5.68×10^{-6}	3.46%	-	62
AGPR-LS	5.85×10^{-6}	1.81%	11	64
Proposed PBAL-LS ($\epsilon = 10\%$)	5.85×10^{-6}	2.28%	10	38

Note: The parameter ϵ in the AGPR-LS method is set to be 0.001.

5.2. Example 2: A quadratic function

The second example considers a quadratic performance function of the form [46]:

$$Y = g(\boldsymbol{X}) = a - X_d + b\sum_{i=1}^{d-1} X_i^2, \tag{27}$$

where $\boldsymbol{X} = [X_1, X_2, \cdots, X_d]$ is a vector of d independent log-normal variables with a mean of 1 and a standard deviation of 0.2. In this example, the dimension is set to be $d = 21$, while the other two parameters are $a = 2.5$ and $b = 0.02$.

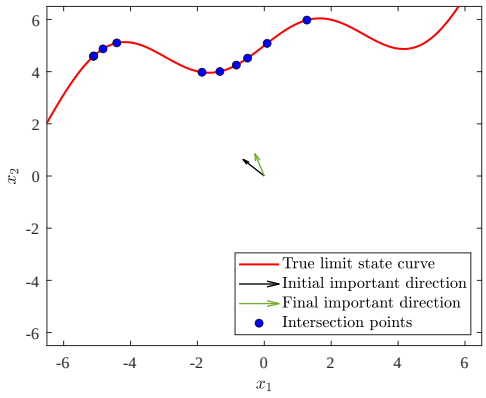

Figure 4: Illustration of the proposed PBAL-LS method ($\epsilon = 10\%$) in Example 1.

The results of several reliability analysis methods are summarized in Table 2. The reference value of the failure probability is 2.00×10^{-8} with a COV being 2.23%, provided by MCS with 10^{11} samples. In order to produce a failure probability estimate with a small COV, both standard LS and CLS requires a large number of lines, as well as $\mathcal{G}$-function calls. The results of AK-IS and AGPR-LS are empty because FORM-HLRF fails in this example. The proposed PBAL-LS is able to produce an accurate failure probability estimate with only 39 additional lines and a total of 137 performance function evaluations.

Table 2: Reliability results for Example 2 obtained from several methods.

Method	$\hat{P}_f$	$\mathrm{COV}[\hat{P}_f]$ or $\overline{\mathrm{COV}}[\hat{P}_f]$	N_{line}	N_{total}
MCS	2.00×10^{-8}	2.23%	-	10^{11}
Standard LS	2.01×10^{-8}	7.64%	100	422
	2.04×10^{-8}	4.88%	200	822
CLS	1.94×10^{-8}	7.31%	100	486
	2.17×10^{-8}	4.82%	200	918
AK-IS	-	-	-	-
AGPR-LS	-	-	-	-
Proposed PBAL-LS ($\epsilon = 10\%$)	1.95×10^{-8}	8.38%	39	137

5.3. Example 3: A nonlinear oscillator

As a third example, we consider a nonlinear single-degree-of-freedom (SDOF) oscillator under a rectangular-pulse load [47], which is shown in Fig. 5. The limit state function is defined by:

$$Y = g\left(m, c_1, c_2, r, F_1, t_1\right) = 3r - \left| \frac{2F_1}{c_1 + c_2} \sin\left(\frac{t_1}{2} \sqrt{\frac{c_1 + c_2}{m}} \right) \right|, \tag{28}$$

where m, c_1, c_2, r, F_1, t_1 are six random variables, which are specified according to Table 3.

The reference failure probability of this example is taken as 1.15×10^{-7} with COV being 2.94%, provided by the MCS method with 10^{10} samples. Table 4 summarizes the results by several other LS methods, along those of MCS. It is seen that with the same number of lines the CLS method is able to give much more better failure probability estimate with a smaller COV than the standard LS method, but at the expense of sightly increased $\mathcal{G}$-function evaluations. Note that both the two methods require considerably more calls to the $\mathcal{G}$-function than AK-IS, AGPR-LS and PBAL-LS in order to achieve a desired level of accuracy, especially for the standard LS method. AK-IS and AGPR-LS method are still much less efficient than the proposed PBAL-LS method in terms of N_{total}, even though they give very similar estimates for the failure probability.

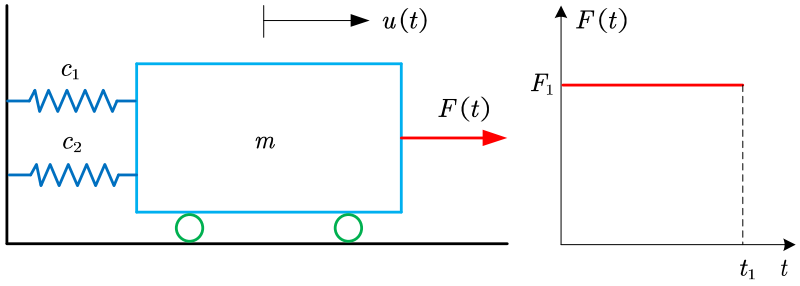

Figure 5: A nonlinear SDOF oscillator subject to pulse load.

5.4. Example 4: A cantilever tube

The third example consists of a cantilever tube subject to three forces and one torque [48], as shown in Fig. 6. The performance function is defined as

$$Y = S_y - \sigma_{\max}, \tag{29}$$

Table 3: Random variables for Example 3.

Variable		Distribution	Mean	COV
m	Mass	Normal	1.0	0.10
c_1	Stiffness	Lognormal	1.0	0.10
c_2	Stiffness	Lognormal	0.1	0.10
r	Yield displacement	Normal	0.5	0.10
F_1	Load amplitude	Lognormal	0.4	0.20
t_1	Load duration	Normal	1.0	0.20

where S_y is the yield stress of the material; $\sigma_{\max}$ denotes the maximum von Mises tress on the top surface of the tube at the origin, which is given by:

$$\sigma_{\max} = \sqrt{\sigma_x^2 + 3\tau_{zx}^2} \tag{30}$$

where σ_x and τ_{zx} read:

$$\sigma_x = \frac{P + F_1 \sin\theta_1 + F_2 \sin\theta_2}{A} + \frac{d\left(F_1 L_1 \cos\theta_1 + F_2 L_2 \cos\theta_2\right)}{2I} \tag{31}$$

$$\tau_{zx} = \frac{Td}{2J} \tag{32}$$

with

$$A = \frac{\pi}{4}\left[d^2 - (d-2t)^2\right], \tag{33}$$

$$I = \frac{\pi}{64}\left[d^4 - (d-2t)^4\right], \tag{34}$$

$$J = 2I. \tag{35}$$

There are a total number of 11 random variables involved in this example, as listed in Table 5.

Table 6 compares the results of several reliability analysis methods. The reference value of the failure probability is 5.99×10^{-8} with COV being 1.29%, which is provided by the MCS method with 10^{11} samples. Both standard LS and CLS results in large COVs even using 1000 lines in this example. The number of $\mathcal{G}$-function calls can be significantly reduced by applying AK-IS and AGPR-LS and PBAL-LS. Among them, the proposed method performs much better in terms of N_{tobal}.

Table 4: Reliability results for Example 3 obtained from several methods.

Method	$\hat{P}_f$	COV$[\hat{P}_f]$ or $\overline{\text{COV}}[\hat{P}_f]$	N_{line}	N_{total}
MCS	1.15×10^{-7}	2.94%	-	10^{10}
Standard LS	6.57×10^{-8}	17.14%	500	1969
	9.29×10^{-8}	13.54%	1000	3909
CLS	1.17×10^{-7}	5.89%	500	2084
	1.14×10^{-7}	2.76%	1000	4113
AK-IS	1.12×10^{-7}	2.61%	-	156
AGPR-LS	1.14×10^{-7}	0.86%	46	103
Proposed PBAL-LS ($\epsilon = 10\%$)	1.17×10^{-7}	7.62%	17	62

Note: The parameter ϵ in the AGPR-LS method is set to be 0.005.

5.5. Example 5: A transmission tower

The last example involves a transmission tower subjected to lateral loads (as shown in Fig. 7), which is modified from [49, 43]. With the aid of a finite-element software called OpenSees, the tower is modelled as a three-dimensional nonlinear truss structure consisting of 24 nodes and 80 truss members. The geometric dimensions of the finite element model are shown in Fig. 7(a). For each member, the cross-sectional area is the same, denoted by A. The uniaxial Giuffrè-Menegotto-Pinto material law (Steel02 in OpenSees) is adopted, as schematically depicted in Fig. 7(c). At least six parameters are needed for the Steel02 model, i.e., Fy, E_0, b, $R0$, $CR1$ and $CR2$. The detailed description of these parameters can be found in the command manual of OpenSees. In this study, the last three parameters are specified as: $R0 = 10$, $CR1 = 0.925$ and $CR2 = 0.15$. Ten lateral loads, P_1-P_{10}, are applied to the structure along the x-axis (see Fig. 7(a)). The performance function is defined as follows:

$$Y = g(P_1\text{-}P_{10}, A, E_0, F_y, b) = \Delta - \frac{u_{1,x} + u_{2,x}}{2}, \tag{36}$$

where Δ is a threshold, specified as 100 mm; $u_{1,x}$ and $u_{2,x}$ represent the horizontal displacements of nodes 1 and 2 (see Fig. 7(b)), respectively. $u_{1,x}$ is a function of the 14 random variables described in Table 7, and

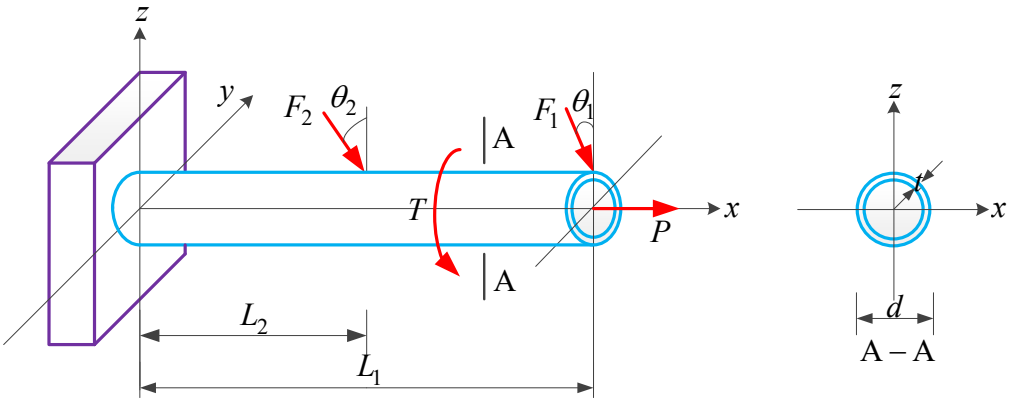

Figure 6: A cantilever tube subject to three forces and one torsion.

so is $u_{2,x}$.

In this example, we cannot afford to perform the MCS method for providing a reference solution. Alternatively, the IS method provided in UQLab [50] is used due to its improved efficiency for an expensive reliability analysis. The failure probability estimate from IS is 5.56×10^{-8} with a COV being 1.00%. The results of IS are reported in Table 8, along with those of some other methods. The standard LS, CLS, AK-IS, and AGPR-LS methods produce errors or fail to converge on multiple trivals, so their results are not available. On the contrary, the proposed PBAL-LS method can still work and produce reasonable results with only 112 $\mathcal{G}$-function evaluations.

Table 5: Random variables for Example 4.

Variable	Distribution	Mean	COV
t	Normal	5 mm	0.05
d	Normal	40 mm	0.05
L_1	Normal	120 mm	0.05
L_2	Normal	60 mm	0.05
F_1	Lognormal	2.0 kN	0.15
F_2	Lognormal	1.5 kN	0.15
P	Lognormal	10 kN	0.20
T	Lognormal	0.2 N·m	0.15
S_y	Normal	300 MPa	0.10
θ_1	Normal	10°	0.05
θ_2	Normal	10°	0.05

Table 6: Reliability results for Example 4 obtained from several methods.

Method	$\hat{P}_f$	$\mathrm{COV}[\hat{P}_f]$ or $\overline{\mathrm{COV}}[\hat{P}_f]$	N_{line}	N_{total}
MCS	5.99×10^{-8}	1.29%	-	10^{11}
Standard LS	6.62×10^{-8}	15.71%	500	1960
	4.71×10^{-8}	11.72%	1000	3944
CLS	4.47×10^{-8}	10.31%	500	2342
	5.59×10^{-8}	11.22%	1000	4882
AK-IS	5.91×10^{-8}	2.80%	-	481
AGPR-LS	5.88×10^{-8}	1.18%	107	211
Proposed PBAL-LS ($\epsilon = 10\%$)	5.92×10^{-8}	9.16%	60	175

Note: The parameter ϵ in the AGPR-LS method is set to be 1.

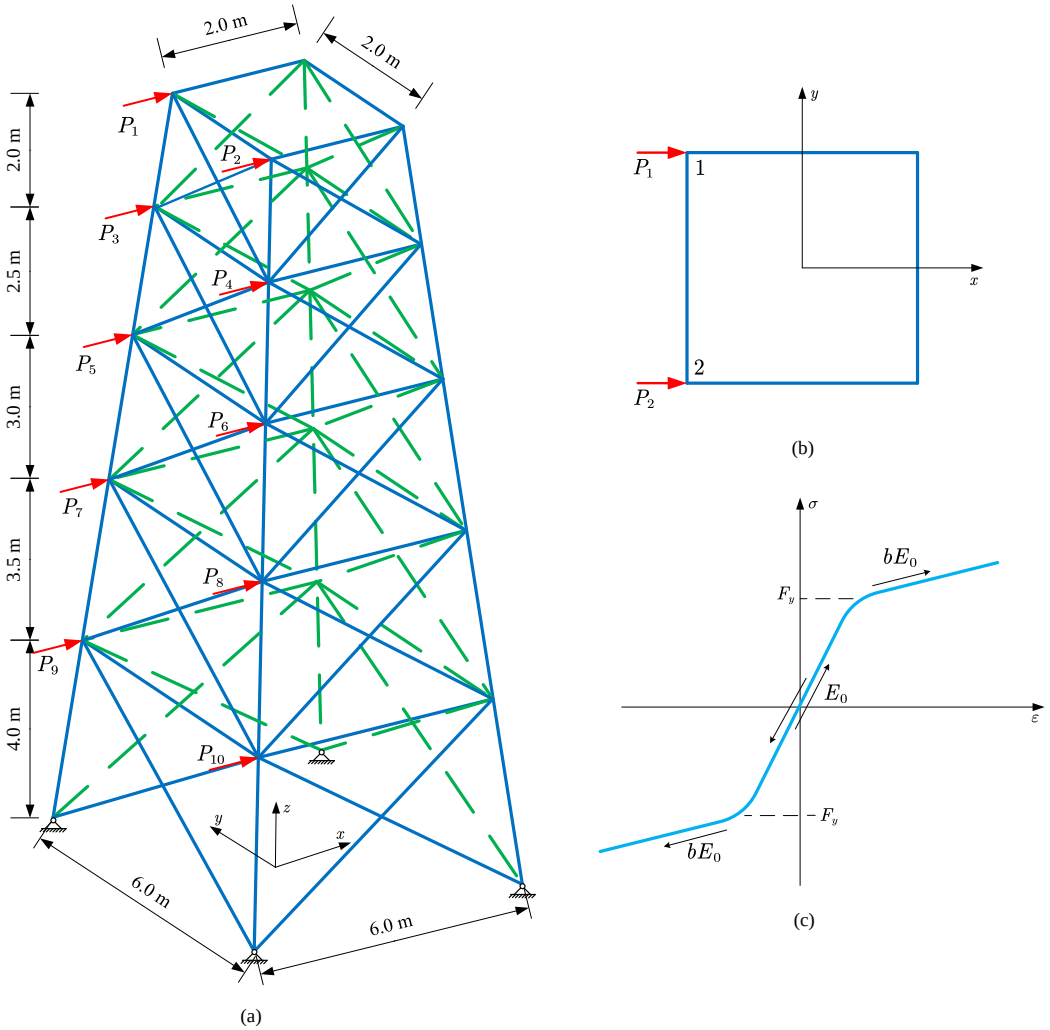

Figure 7: A transmission tower subject to horizontal loads.

Table 7: Random variables for Example 5.

Variable	Distribution	Mean	COV
P_1, P_2	Lognormal	10 kN	0.20
P_3, P_4	Lognormal	8 kN	0.20
P_5, P_6	Lognormal	6 kN	0.20
P_7, P_8	Lognormal	4 kN	0.20
P_9, P_{10}	Lognormal	2 kN	0.20
A	Normal	5000 mm^2	0.05
E_0	Normal	200 GPa	0.15
F_y	Normal	400 Mpa	0.15
b	Uniform	0.02	0.05

Table 8: Reliability results for Example 5 obtained from several methods.

Method	$\hat{P}_f$	COV$[\hat{P}_f]$ or $\overline{\text{COV}}[\hat{P}_f]$	N_{line}	N_{total}
IS	5.56×10^{-8}	1.00%	-	61,430
Standard LS	-	-	-	-
CLS	-	-	-	-
AK-IS	-	-	-	-
AGPR-LS	-	-	-	-
Proposed PBAL-LS ($\epsilon = 10\%$)	5.57×10^{-8}	9.36%	40	112

6. Conclusions

This paper presents a 'partially Bayesian active learning line sampling ' (PBAL-LS) method for structural reliability analysis, especially when involving small failure probabilities. The proposed method is derived from the Bayesian interpretation of the failure probability integral in the LS method, in which the discretization error is regarded as a kind of epistemic uncertainty that can be modeled explicitly. By assigning a Gaussian process prior over the β-function, the induced posterior statistics of the failure probability conditional on observations is then obtained. Two essential components for active learning, i.e., learning function and stopping criterion, are proposed by taking advantage of the uncertainty representation of the failure probability. In addition to these theoretical developments, we also design a tailored algorithm for the PBAL-LS method, which allows updating the important direction on the fly and efficiently processing the lines. Five numerical studies indicate that the proposed method outperforms several existing LS methods in one or more aspects of efficiency, accuracy and robustness when assessing extremely small failure probabilities in the order of $10^{-6} - 10^{-8}$.

While the application scope of the proposed method is large, it is mostly suitable for assessing (small) failure probabilities of weakly or moderately nonlinear problems in low-to-medium dimensions, where a single main failure domain exits. The proposed method might also be extended to cases with multiple failure domains if multiple initial important directions can be identified and updated. This will be investigated in the future work.

Declaration of competing interest

The authors declare that they have no known competing financial interests or personal relationships that could have appeared to influence the work reported in this paper.

Acknowledgments

Chao Dang is mainly supported by China Scholarship Council (CSC). Jingwen Song acknowledges the financial support from the National Natural Science Foundation of China (grant no. 12202358 and

12220101002). Pengfei Wei is grateful to the support from the National Natural Science Foundation of China (grant no. 51905430 and 72171194). Chao Dang, Pengfei Wei and Michael Beer also would like to appreciate the support of Sino-German Mobility Program under grant number M-0175.

Data availability

Data will be made available on request.

References

[1] A. M. Freudenthal, Safety and the probability of structural failure, Transactions of the American Society of Civil Engineers 121 (1) (1956) 1337–1375. doi:https://doi.org/10.1061/TACEAT.0007306.

[2] M. Shinozuka, Monte Carlo solution of structural dynamics, Computers & Structures 2 (5-6) (1972) 855–874. doi:https://doi.org/10.1016/0045-7949(72)90043-0.

[3] R. Melchers, Importance sampling in structural systems, Structural Safety 6 (1) (1989) 3–10. doi:https://doi.org/10.1016/0167-4730(89)90003-9.

[4] S. Engelund, R. Rackwitz, A benchmark study on importance sampling techniques in structural reliability, Structural Safety 12 (4) (1993) 255–276. doi:https://doi.org/10.1016/0167-4730(93)90056-7.

[5] R. E. Melchers, Structural system reliability assessment using directional simulation, Structural Safety 16 (1-2) (1994) 23–37. doi:https://doi.org/10.1016/0167-4730(94)00026-M.

[6] S.-K. Au, J. L. Beck, Estimation of small failure probabilities in high dimensions by subset simulation, Probabilistic Engineering Mechanics 16 (4) (2001) 263–277. doi:https://doi.org/10.1016/S0266-8920(01)00019-4.

[7] S.-K. Au, Y. Wang, Engineering risk assessment with subset simulation, John Wiley & Sons, 2014.

[8] P.-S. Koutsourelakis, H. J. Pradlwarter, G. I. Schueller, Reliability of structures in high dimensions, part I: algorithms and applications, Probabilistic Engineering Mechanics 19 (4) (2004) 409–417. doi:https://doi.org/10.1016/j.probengmech.2004.05.001.

[9] P.-S. Koutsourelakis, Reliability of structures in high dimensions. part II. theoretical validation, Probabilistic Engineering Mechanics 19 (4) (2004) 419–423. doi:https://doi.org/10.1016/j.probengmech.2004.05.002.

[10] B. J. Bichon, M. S. Eldred, L. P. Swiler, S. Mahadevan, J. M. McFarland, Efficient global reliability analysis for nonlinear implicit performance functions, AIAA Journal 46 (10) (2008) 2459–2468. doi:https://doi.org/10.2514/1.34321.

[11] B. Echard, N. Gayton, M. Lemaire, AK-MCS: an active learning reliability method combining Kriging and Monte Carlo simulation, Structural Safety 33 (2) (2011) 145–154. doi:https://doi.org/10.1016/j.strusafe.2011.01.002.

[12] P. Koutsourelakis, H. Pradlwarter, G. Schuëller, Reliability of structures in high dimensions, in: PAMM: Proceedings in Applied Mathematics and Mechanics, Vol. 3, Wiley Online Library, 2003, pp. 495–496. doi:https://doi.org/10.1002/pamm.200310517.

[13] M. Hohenbichler, R. Rackwitz, Improvement of second-order reliability estimates by importance sampling, Journal of Engineering Mechanics 114 (12) (1988) 2195–2199. doi:https://doi.org/10.1061/(ASCE)0733-9399(1988)114:12(2195).

[14] H. Pradlwarter, M. Pellissetti, C. Schenk, G. Schueller, A. Kreis, S. Fransen, A. Calvi, M. Klein, Realistic and efficient reliability estimation for aerospace structures, Computer Methods in Applied Mechanics and Engineering 194 (12-16) (2005) 1597–1617. doi:https://doi.org/10.1016/j.cma.2004.05.029.

[15] M. Pellissetti, G. Schuëller, H. Pradlwarter, A. Calvi, S. Fransen, M. Klein, Reliability analysis of spacecraft structures under static and dynamic loading, Computers & Structures 84 (21) (2006) 1313–1325. doi:https://doi.org/10.1016/j.compstruc.2006.03.009.

[16] L. Hinke, L. Pichler, H. Pradlwarter, B. Mace, T. Waters, Modelling of spatial variations in vibration analysis with application to an automotive windshield, Finite Elements in Analysis and Design 47 (1) (2011) 55–62. doi:https://doi.org/10.1016/j.finel.2010.07.013.

[17] E. Zio, N. Pedroni, Functional failure analysis of a thermal–hydraulic passive system by means of line sampling, Reliability Engineering & System Safety 94 (11) (2009) 1764–1781. doi:https://doi.org/10.1016/j.ress.2009.05.010.

[18] E. Zio, N. Pedroni, An optimized line sampling method for the estimation of the failure probability of nuclear passive systems, Reliability Engineering & System Safety 95 (12) (2010) 1300–1313. doi:https://doi.org/10.1016/j.ress.2010.06.007.

[19] H. Pradlwarter, G. I. Schueller, P.-S. Koutsourelakis, D. C. Charmpis, Application of line sampling simulation method to reliability benchmark problems, Structural Safety 29 (3) (2007) 208–221. doi:https://doi.org/10.1016/j.strusafe.2006.07.009.

[20] L. S. Katafygiotis, J. Wang, Reliability analysis of wind-excited structures using domain decomposition method and line sampling, Structural Engineering and Mechanics 32 (1) (2009) 37–53. doi:https://doi.org/10.12989/sem.2009.32.1.037.

[21] E. Patelli, COSSAN: A multidisciplinary software suite for uncertainty quantification and risk management, in: Handbook of Uncertainty Quantification, Springer International Publishing Switzerland, 2017, pp. 1909–1977. doi:https://dx.doi.org/10.1007/978-3-319-11259-6_59-1.

[22] Z. Lu, S. Song, Z. Yue, J. Wang, Reliability sensitivity method by line sampling, Structural Safety 30 (6) (2008) 517–532. doi:https://doi.org/10.1016/j.strusafe.2007.10.001.

[23] M. A. Valdebenito, H. A. Jensen, H. Hernández, L. Mehrez, Sensitivity estimation of failure probability applying line sampling, Reliability Engineering & System Safety 171 (2018) 99–111. doi:https://doi.org/10.1016/j.ress.2017.11.010.

[24] M. A. Valdebenito, H. B. Hernández, H. A. Jensen, Probability sensitivity estimation of linear stochastic finite element models applying line sampling, Structural Safety 81 (2019) 101868. doi:https://doi.org/10.1016/j.strusafe.2019.06.002.

[25] X. Zhang, Z. Lu, W. Yun, K. Feng, Y. Wang, Line sampling-based local and global reliability sensitivity analysis, Structural and Multidisciplinary Optimization 61 (1) (2020) 267–281. doi:https://doi.org/10.1007/s00158-019-02358-9.

[26] X. Yuan, Z. Zheng, B. Zhang, Augmented line sampling for approximation of failure probability function in reliability-based analysis, Applied Mathematical Modelling 80 (2020) 895–910. doi:https://doi.org/10.1016/j.apm.2019.11.009.

[27] M. de Angelis, E. Patelli, M. Beer, Advanced line sampling for efficient robust reliability analysis, Structural Safety 52 (2015) 170–182. doi:https://doi.org/10.1016/j.strusafe.2014.10.002.

[28] J. Song, M. Valdebenito, P. Wei, M. Beer, Z. Lu, Non-intrusive imprecise stochastic simulation by line sampling, Structural Safety 84 (2020) 101936. doi:https://doi.org/10.1016/j.strusafe.2020.101936.

[29] J. Song, P. Wei, M. Valdebenito, M. Beer, Adaptive reliability analysis for rare events evaluation with global imprecise line sampling, Computer Methods in Applied Mechanics and Engineering 372 (2020) 113344. doi:https://doi.org/10.1016/j.cma.2020.113344.

[30] J. Wang, Z. Lu, Y. Cheng, L. Wang, An efficient method for estimating failure probability bound functions of composite structure under the random-interval mixed uncertainties, Composite Structures (2022) 116011doi:https://doi.org/10.1016/j.compstruct.2022.116011.

[31] M. A. Shayanfar, M. A. Barkhordari, M. Barkhori, M. Rakhshanimehr, An adaptive line sampling method for reliability analysis, Iranian Journal of Science and Technology, Transactions of Civil Engineering 41 (3) (2017) 275–282. doi:https://doi.org/10.1007/s40996-017-0070-3.

[32] I. Papaioannou, D. Straub, Combination line sampling for structural reliability analysis, Structural Safety 88 (2021) 102025. doi:https://doi.org/10.1016/j.strusafe.2020.102025.

[33] M. A. Valdebenito, P. Wei, J. Song, M. Beer, M. Broggi, Failure probability estimation of a class of series systems by multidomain line sampling, Reliability Engineering & System Safety 213 (2021) 107673. doi:https://doi.org/10.1016/j.ress.2021.107673.

[34] Z. Lv, Z. Lu, P. Wang, A new learning function for kriging and its applications to solve reliability problems in engineering, Computers & Mathematics with Applications 70 (5) (2015) 1182–1197. doi:https://doi.org/10.1016/j.camwa.2015.07.004.

[35] I. Depina, T. M. H. Le, G. Fenton, G. Eiksund, Reliability analysis with metamodel line sampling, Structural Safety 60 (2016) 1–15. doi:https://doi.org/10.1016/j.strusafe.2015.12.005.

[36] J. Song, P. Wei, M. Valdebenito, M. Beer, Active learning line sampling for rare event analysis, Mechanical Systems and Signal Processing 147 (2021) 107113. doi:https://doi.org/10.1016/j.ymssp.2020.107113.

[37] M. A. Valdebenito, M. de Angelis, E. Patelli, Line sampling simulation: Recent advancements and applications, in:

Reliability-Based Analysis and Design of Structures and Infrastructure, CRC Press, 2021, pp. 215–226. doi:https://doi.org/10.1201/9781003194613-15.

[38] G. I. Schueller, H. J. Pradlwarter, P.-S. Koutsourelakis, A critical appraisal of reliability estimation procedures for high dimensions, Probabilistic Engineering Mechanics 19 (4) (2004) 463–474. doi:https://doi.org/10.1016/j.probengmech.2004.05.004.

[39] A. O'Hagan, Bayes–Hermite quadrature, Journal of Statistical Planning and Inference 29 (3) (1991) 245–260. doi:https://doi.org/10.1016/0378-3758(91)90002-V.

[40] C. E. Rasmussen, Z. Ghahramani, Bayesian Monte Carlo, Advances in Neural Information Processing Systems (2003) 505–512.

[41] C. E. Rasmussen, C. K. Williams, Gaussian processes for machine learning, The MIT press, 2006.

[42] D. B. Owen, A table of normal integrals: A table, Communications in Statistics-Simulation and Computation 9 (4) (1980) 389–419. doi:https://doi.org/10.1080/03610918008812164.

[43] C. Dang, M. A. Valdebenito, M. G. Faes, P. Wei, M. Beer, Structural reliability analysis: A Bayesian perspective, Structural Safety 99 (2022) 102259. doi:https://doi.org/10.1016/j.strusafe.2022.102259.

[44] B. Echard, N. Gayton, M. Lemaire, N. Relun, A combined importance sampling and kriging reliability method for small failure probabilities with time-demanding numerical models, Reliability Engineering & System Safety 111 (2013) 232–240. doi:https://doi.org/10.1016/j.ress.2012.10.008.

[45] A. M. Hasofer, N. C. Lind, Exact and invariant second-moment code format, Journal of the Engineering Mechanics Division 100 (1) (1974) 111–121. doi:https://doi.org/10.1061/JMCEA3.0001848.

[46] J. Xu, F. Kong, A new unequal-weighted sampling method for efficient reliability analysis, Reliability Engineering & System Safety 172 (2018) 94–102. doi:https://doi.org/10.1016/j.ress.2017.12.007.

[47] C. G. Bucher, U. Bourgund, A fast and efficient response surface approach for structural reliability problems, Structural Safety 7 (1) (1990) 57–66. doi:https://doi.org/10.1016/0167-4730(90)90012-E.

[48] X. Du, Unified uncertainty analysis by the first order reliability method, Journal of Mechanical Design 130 (9), 091401 (08 2008). doi:https://doi.org/10.1115/1.2943295.

[49] C. Dang, P. Wei, M. G. Faes, M. A. Valdebenito, M. Beer, Interval uncertainty propagation by a parallel Bayesian global optimization method, Applied Mathematical Modelling 108 (2022) 220–235. doi:https://doi.org/10.1016/j.apm.2022.03.031.

[50] S. Marelli, R. Schöbi, B. Sudret, UQLab user manual – Structural reliability (Rare event estimation), Tech. rep., Chair of Risk, Safety and Uncertainty Quantification, ETH Zurich, Switzerland, report UQLab-V2.0-107 (2022).